Available online at www.sciencedirect.com
ScienceDirect
Carbon 45 (2007) 1482–1491
CARBON
www.elsevier.com/locate/carbon

A first principles study of the optical properties of B_xC_y single wall nanotubes

Debnarayan Jana [a,*], Li-Chyong Chen [b,*], Chun Wei Chen [c], Surojit Chattopadhyay [d], Kuei-Hsien Chen [d]

[a] Department of Physics, University College of Science and Technology, University of Calcutta, Kolkata 700 009, West Bengal, India
[b] Center for Condensed Matter Sciences, National Taiwan University, Taipei 106, Taiwan
[c] Department of Material Science and Engineering, National Taiwan University, Taipei 106, Taiwan
[d] Institute of Atomic and Molecular Sciences, Academia Sinica, Taipei 106, Taiwan

Received 19 June 2006; accepted 9 March 2007
Available online 16 March 2007

Abstract

The optical properties of small radius (<1 nm) single wall carbon nanotubes (SWCNTs) alloyed with boron were examined using relaxed C–C bond length ab initio calculations in the long wavelength limit. The magnitude of the static dielectric constant essentially depends on the B concentration as well as the direction of polarization. The maximum value of the absorption coefficient is shown to strongly depend on the concentration of B in a non-linear way with a minimum at a critical concentration of 0.40 for both the parallel polarization and the un-polarized cases and of 0.29 for perpendicular polarization of the electromagnetic field. The peak of the loss function in parallel polarization and unpolarized cases shifts to a lower frequency with increasing concentration up to 50% but then shifts to a higher frequency. The non-linear fits to the plasma resonance frequency variation with B concentration indicate the existence of a unique minimum. All these factors may shed light on the nature of collective excitations in B-alloyed SWCNTs.

1. Introduction

Carbon nanotubes (CNTs) because of to their unique one-dimensional structure and unusual physical, chemical and mechanical properties have attracted the attention of theoretical and experimental research groups [1,2]. The electronic properties of single wall carbon nanotubes (SWCNTs) can be tailored [3,4] by substituting carbon atom(s) by heteroatoms (s) such as boron or nitrogen. It is well known that pure CNTs are unable to detect highly toxic gases, water molecules and biomolecules [5]. To improve the nanosensor reliability and quality, the importance of substitutional alloying of impurity atoms such as boron, nitrogen have been discussed [6]. In fact, a calculation on the chemical interaction reveals that the boron doped CNT can act as a novel sensor [7] for formaldehyde. The synthesis of composite $B_xC_yN_z$ tubes has been performed and their energy loss spectroscopies have been reported [8,9]. In general, through the reaction with B_2O_3 with CNTs under an Ar atmosphere [10] B atom(s) can be substituted for the carbon atoms(s) of SWNT. In literature, the synthesis and electronic properties of B-substituted SWCNT have been discussed [11,12]. A quantum chemical calculation [13] has been employed to investigate the larger mobility (i.e. electronic conductivity) of B and N doped CNTs. Recently, the electronic structure and optical properties of B doped single wall carbon nanotubes (SWCNTs) have been studied in detail and it is found that boron is in sp^2 configuration [14]. It has also been shown recently that even a small amount dopant can significantly change the mesoscopic conductivity [15] of chemically B doped CNTs. The electron current distribution in B and N doped armchair CNT have been investigated [16] using

* Corresponding authors. Fax: +91 (0) 3323509755 (D. Jana); fax: +886 2 23655405 (L.-C. Chen).
E-mail addresses: djphy@caluniv.ac.in (D. Jana), chenlc@ntu.edu.tw (L.-C. Chen).

0008-6223/$ - see front matter © 2007 Elsevier Ltd. All rights reserved.
doi:10.1016/j.carbon.2007.03.024

DFT and Green's function to show a chiral flow of current. All the above examples eventually indicate the importance of the study of B doped CNTs and invite further investigation about the optical properties of the doped system as a function of B concentration. Since this doping can alter the band structure of SWCNTs (such as band gap, the density of states near Fermi energy) considerably [17,18], we would naturally expect some dramatic changes in the response of the B_xC_y nanotubes under an electromagnetic field. As a matter of fact, in recent years the spectroscopic studies of BC_3 SWNTs have been interpreted in terms of ab initio band structure calculation [19,20].

The optical properties of 4 Å diameter pure SWCNT have been investigated [21–23] recently by first principles calculation to explain the experimental results. Most recently, ab initio calculations of the linear and non-linear optical properties of pure CNTs have shown that [24] the dielectric function depends essentially on chirality, diameter and the nature of polarizations of incident electromagnetic field. In this paper, we study the response of the B alloyed CNTs (pure metallic, semiconductor and quasi-metallic) under the action of a uniform electric field with various polarizations direction through relaxed C–C bond length ab initio density functional theory (DFT) calculations. The geometrical structure of impure system was built by replacing one of the carbon atom(s) in the hexagonal ring by B atom(s). The preferred boron sites were chosen having lowest total energy. In this first principles computation, we have only *one* fixed parameter from the experiment namely the carbon–carbon bond length (0.142 nm) for pure SWCNT. In particular, we concentrate on the static long wavelength ($\omega \to 0$, $q \to 0$) optical response of the system apart from its variation with frequency and discuss the nature of its variation with chemical doping of B concentration in a semiconductor (8,0) nanotube.

2. Numerical methods

The optical properties of any system are generally studied by the complex dielectric function defined by $\vec{D}(\omega) = \varepsilon(\omega)\vec{E}(\omega) = [\varepsilon_1(\omega) + i\varepsilon_2(\omega)]\vec{E}(\omega)$. However, $\varepsilon_1(\omega)$ and $\varepsilon_2(\omega)$ are not independent of each other. In this numerical simulation, the imaginary part of the dielectric function has been computed by using first-order time dependent perturbation theory. In the simple dipole approximation used in CASTEP code [25], the imaginary part is given by

$$\varepsilon_2(q \to 0_{\vec{u}}, \hbar\omega) = \frac{2e^2\pi}{\Omega\varepsilon_0} \sum_{k,V,C} |\langle \psi_k^C | \vec{u} \cdot \vec{r} | \psi_k^V \rangle|^2 \delta(E_k^C - E_k^V - E) \quad (1)$$

Ω and ε_0 represent respectively the volume of the super-cell and the dielectric constant of the free space. The sum over k is a crucial point in numerical calculation. It actually samples the whole region of Brillouin zone (BZ) in the k space. The other two sums take care the contribution of the unoccupied conduction band (CB) and occupied valence band (VB). In computing the above dielectric function, typically [1/2 (total number of electrons + 4] no. of bands were taken. Here, $\vec{u}, \vec{r}$ respectively represent the polarization vector of the incident electric field and position vector. The matrix element of this dot product of these two vectors is computed between the single electron energy eigen states. Since the magnetic field effect is weaker by a factor of v/c, the transition matrix elements between the eigenstates of CB and VB have been calculated only due to the electric field. No phonon contribution is taken into account here. Moreover, in this formulation, the local field effect and the excitonic effect have been neglected.

To determine the wave functions in Eq. (1), we perform the first principles spin unpolarized density functional theory using plane wave pseudo-potential methods [26,27]. Like any ab initio calculation, the self-consistent Kohn Sham (KS) equation has been used to compute the eigen function here. For the exchange and correlation term, the generalized gradient approximation (GGA) as proposed by Perdew–Berke–Ernzerhof [28] is adopted. The standard norm-conserving pseudo-potential in reciprocal space is invoked for the optical calculation. Compared to the standard local density approximation (LDA) (with appropriate modifications) used mostly in electronic band structure calculation, the optical properties of the system are normally standardized by *spin un-polarized* GGA. A cutoff energy of 470 eV for the grid integration was adopted for computing the charge density. For Brillouin zone (BZ) integration along the tube axis, we have used six Monkhorst [29] k-points. The smearing broadening in computing the optical properties was kept fixed at 0.5 eV. The atomic positions are relaxed until the forces on the atoms are less than 0.01 eV/Å. The typical convergence was achieved till the tolerance in the Fermi energy is 0.1×10^{-6} eV. The typical computational super cell used here (which includes typical four units of CNT) is the 3d triclinic crystal ($a = 18.801$ Å, $b = 19.004$ Å, $c = 4.219$ Å and angles $\alpha = \beta = 90°$, $\gamma = 120°$) having symmetry P1.

3. Results and discussion

3.1. Study of band structure of B_xC_y system

Before we discuss the optical properties, we show in Fig. 1 the typical ball and stick model of pure (8,0) and BC_3 system. All the results presented in this numerical calculation have same set of parameters as indicated in earlier section. In Fig. 2, we schematically show the band structure of BC_3 system respectively. All the energies shown in the diagram have been measured with respect to the Fermi energy. For pure (8,0) we find the Fermi energy 6.028 eV with band gap at Γ point (most symmetric point in the BZ) as 0.48 eV. We also notice that the Fermi energy (the dashed line) is within the valence band and conduction band. However, alloying with Boron atoms in (8,0) nanotubes, the Fermi energy reduces to 4.256 eV with overlapping of the few energies of valence and conduction band. The band gap in this case turns out as 0.43 eV at Γ point, which is smaller than the pure one. With increasing more number of boron atoms in SWNTs, we find for (8,0) B_3C nanotubes, a further reduction of the Fermi energy to 3.614 eV. More interestingly, we note that a significant increase of the overlapping of valence and conduction band in compared to pure as well as BC_3 SWNT. The band gap in this case turns out as 0.58 eV at Γ point, which is larger than the pure one. The band structure of B_3C (not shown in figure) also reveals that near the bottom of the valence band, there is a gap in energy for all values of k-points in BZ. With increase of B doping, this feature is seen to be an integral part of the dispersion relation. The flatness of the band at various k-points seems to contribute significantly to the optical absorption. The partial density of states (PDOS) of (8,0) B_3C carbon nanotubes shown in Fig. 3 indicates a series of spikes in the whole spectrum

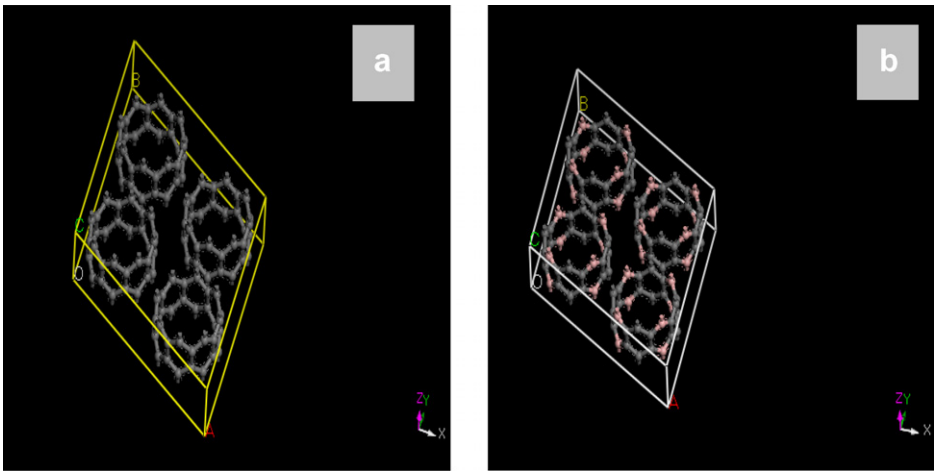

Fig. 1. Ball and stick model of (a) pure (8,0) and (b) BC_3 tube in 3d triclinic structure.

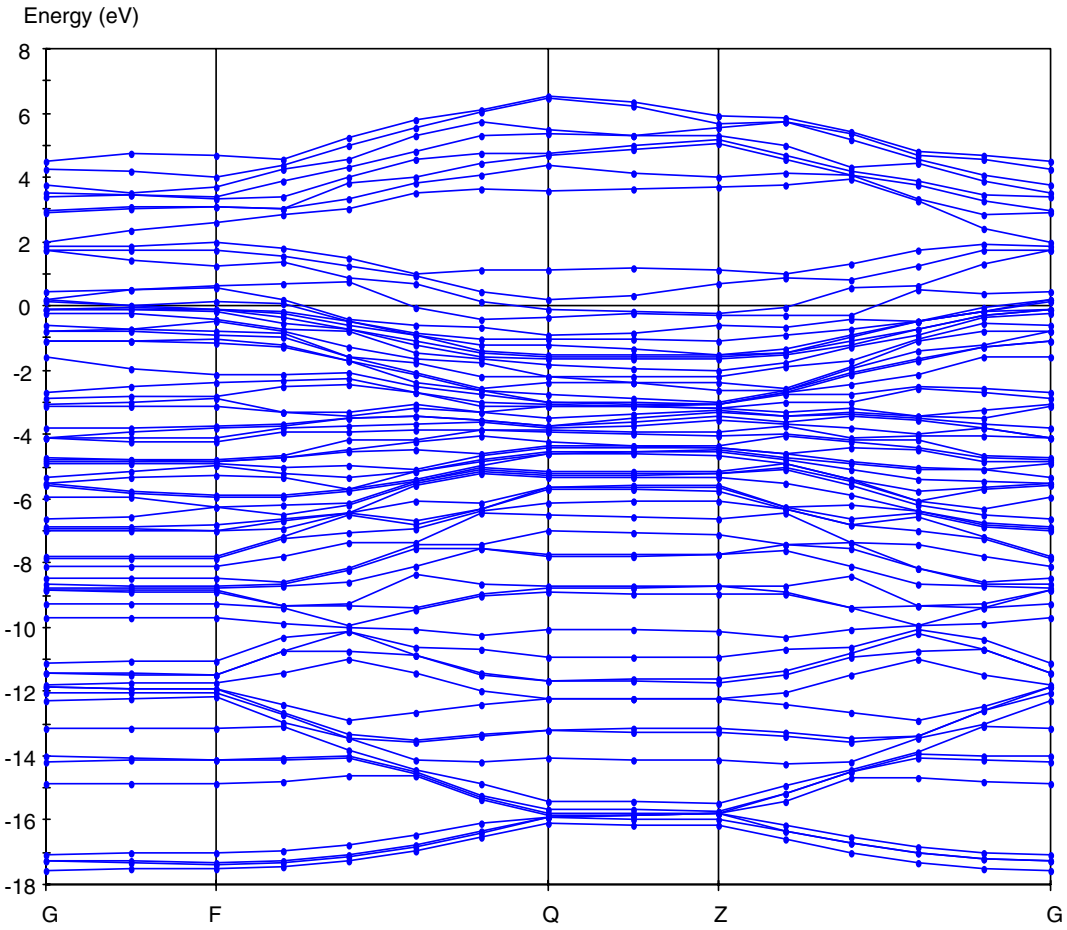

Fig. 2. Band structure of (8,0) BC_3 SWNT. The dashed line is the Fermi energy level.

of band energy and these are basically the van Hove singularity typical characteristics of low dimensional condensed matter systems. The low temperature scanning tunneling spectroscopy (STS) measurement can be used to verify the position of the spikes. It is seen that in both pure and doped case, the contribution of p electrons in valence band is higher compared to its counter part s electrons. The contribution of s electrons in both the cases in the conduction band is meagre. In B_3C case, the contribution of p electrons at the Fermi level have been increased substantially compared to pure case. In fact, the higher value of DOS at the Fermi level signifies the metallicity character of B_3C. In Fig. 4a, the variation of Fermi energy with B doping is indicated. It is observed that with increase of B doing,

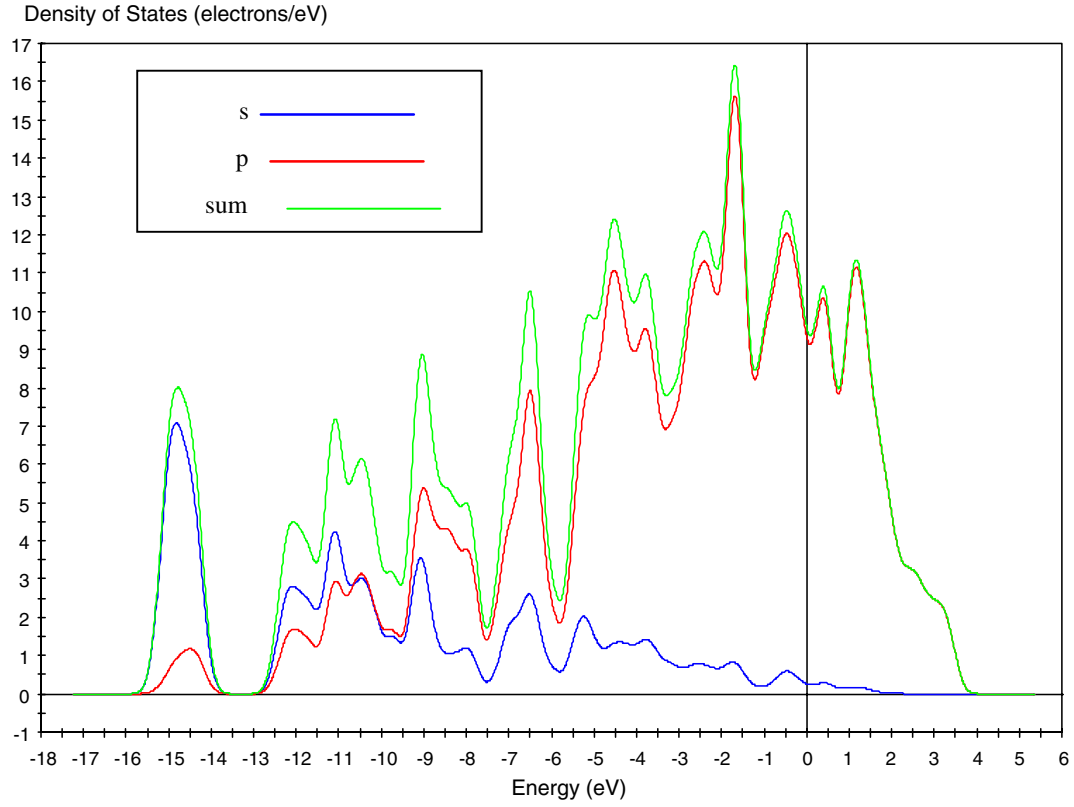

Fig. 3. Partial density of states (PDOS) of (8,0) B_3C SWNT and the dashed line is the position of the Fermi energy level. The energies are measured with respect to this Fermi level.

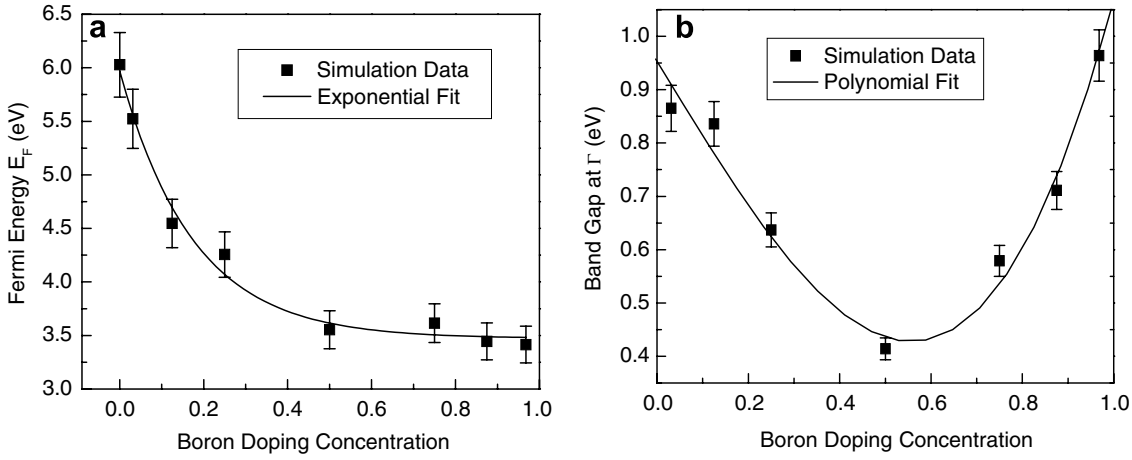

Fig. 4. Variation of Fermi energy with (a) B doping concentration (b) typical variation of the band gap at Γ point with B doping. The energy cut-off, k-point sampling, geometry, GGA/norm-conserving pseudo-potential has been kept constant.

the Fermi Energy *decreases exponentially*. This is understood simply from the fact that the electronic configuration of B atom is $1s^2\ 2s^2 2p^1$. Therefore, doping by B atom always reduces the total no. of electrons N_0 in the system which on the other hand implies the decrease of Fermi energy with B doping. This has also been observed in boron doped multi-walled carbon nanotubes [30,31]. Now, we concentrate here on the band gap in the most symmetric point of the BZ. In Fig. 4b, we show the schematic variation of the band gap at Γ point of the BZ with B doping. A polynomial fit to the data obtained from the band structure calculations reveals that the minimum of the band gap is obtained at some critical doping concentration (~55%). This engineering of band gap at the most symmetric point in BZ may be useful in device and sensor applications. These observations are required later on to understand some of the features of the optical properties of the doped CNT systems.

3.2. Study of dielectric constant of B_xC_y system

We compute the imaginary part of the dielectric constant within the specified frequency range for three types of CNT namely pure metallic, semiconductor and quasi-metallic. It was suggested [21] that because of the presence of the density of scatterers in the super-cell, the imaginary dielectric constant needed to be renormalized. However, we do not account such renormalization in our calculation. Further work is required to justify this renormalization procedure. In Fig. 5, we schematically show the dielectric constant (real as well as imaginary) for both pure (8,0) and BC_3 doped system as a function of frequency. It is evident that in both cases, the imaginary part of the dielectric constant is always positive throughout the range of frequency. This can be understood very simply from Eq. (1) used for this simulation study. The square of the matrix element and the even functional nature of the energy conserving delta function ensure the positivity of ε_2. This property of ε_2 serves as one of the cross-checks in our numerical computation. However, as evident from the figure itself that such a restriction is not obeyed by the real part of the dielectric constant ε_1. We also note that the static value (strictly speaking $\omega \to 0$, but in our numerical computation $\omega = 0.0150$ Hz.) of the dielectric constants for both pure and doped system is always positive. This observation is satisfied by a theorem in continuous media stating that the static electric dielectric constant is always positive [32] for any material in thermal equilibrium. The variation of static dielectric constant with concentration of B has been reported recently [33] to show that a small concentration is enough to change the value drastically from the pure (8,0) SWCNT. It is evident from Fig. 5 that the static value of the dielectric constant (real as well as imaginary) of BC_3 system is higher compared to pure one. The an-isotropic behavior with respect to various flavors of CNT and electro magnetic field is summarized in Tables 1 and 2 in the static values of the dielectric constants of pure and doped system (replacing one of the carbon atom by B atom) at 0.0150 Hz.

We note that the change of value of static dielectric constant depends on both polarizations as well as on the nature of CNT. The parallel polarization refers to the direction of light parallel to the axis of the CNT. For example, in pure case, the static values for parallel polarization for (7,0) and (9,0) are higher than their perpendicular polarization counterparts while the reverse is true for (5,5) and (6,6). For pure metallic tubes (5,5) or (6,6), the doping *increases* the static dielectric constant for parallel polarization but *decreases* its value for perpendicular polarization. The behavior of (7,0) and (10,0) semiconductor CNT is intriguing with respect to doping as well as polarization. In this semiconductor case, the doping *lowers* the static values for parallel as well for unpolarized light while *enhances* the value a small amount in perpendicular situation. In case of semiconducting SWCNT, an ab initio tight-binding calculation [34,35] relates the static value of the dielectric constant with the energy band gap as

Table 1
Un-polarized light with incidence direction (1,0,0)

Nature of CNT/diameter (nm)	Static $\varepsilon_1(\omega)$		Static $\varepsilon_2(\omega)$	
	Pure	Doped	Pure	Doped
(5,5)/0.6783	7.301	8.588	0.059	0.083
(6,6)/0.8140	7.852	10.140	0.229	0.326
(7,0)/0.5483	43.408	28.968	6.278	4.698
(10,0)/0.7833	43.408	26.094	6.790	4.065
(9,0)/0.7049	11.760	72.039	1.006	21.365

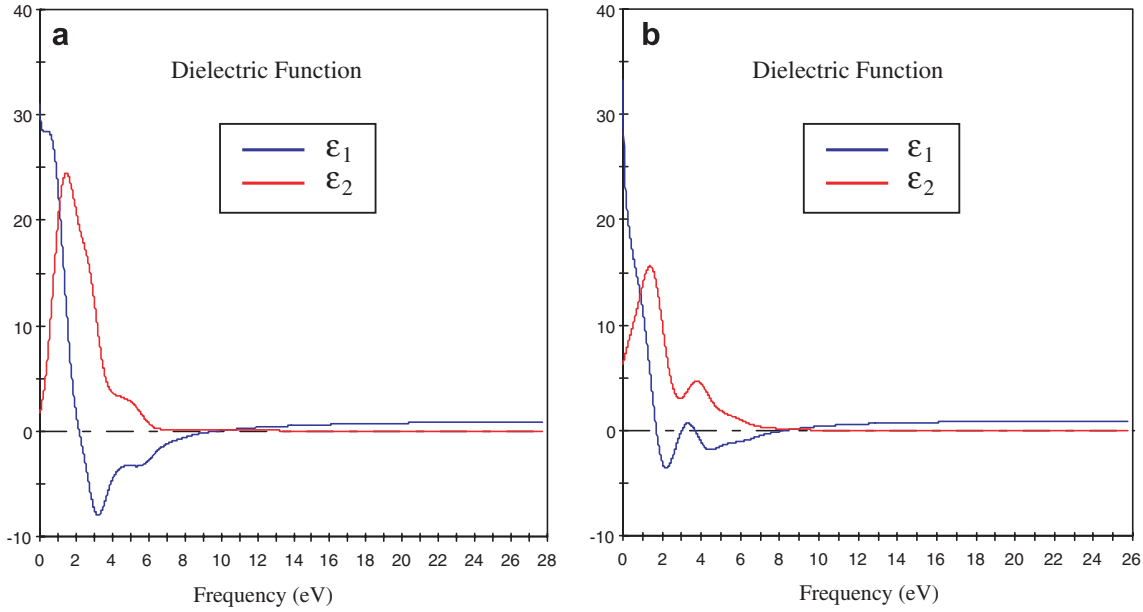

Fig. 5. Typical variation of dielectric constants of (a) pure (8,0) and (b) BC_3 nanotube in parallel polarization as a function of frequency (ω).

Table 2
Parallel polarization and perpendicular polarization

Nature of CNT/diameter (nm)	Parallel polarization				Perpendicular polarization			
	Static $\varepsilon_1(\omega)$		Static $\varepsilon_2(\omega)$		Static $\varepsilon_1(\omega)$		Static $\varepsilon_2(\omega)$	
	Pure	Doped	Pure	Doped	Pure	Doped	Pure	Doped
(5,5)/0.6783	6.487	9.327	0.021	0.081	9.313	8.705	0.199	0.109
(6,6)/0.8140	5.889	11.282	0.016	0.340	11.471	9.836	0.688	0.356
(7,0)/0.5483	77.112	40.982	11.948	6.677	7.752	11.901	0.165	1.097
(10,0)/0.7833	78.582	40.146	13.321	6.737	9.802	11.947	0.422	1.164
(9,0)/0.7049	16.596	132.391	1.686	41.321	5.571	10.341	0.142	0.978

Table 3
Study of minima of α_{max}

Polarization	Minimum value of α_{max} (m^{-1})	Respective boron doping concentration
Parallel	6.48×10^6	0.400
Perpendicular	8.53×10^6	0.290
Unpolarized	7.95×10^6	0.400

$$\varepsilon_1(0) = 1 + \frac{(\hbar\omega_p)^2}{(5.4E_g)^2} \quad (2)$$

Here ω_p is the plasma frequency and E_g is the energy band gap. Based on this equation, a strong upper bound [36] to the static dielectric constant of a semiconductor SWCNT was suggested as

$$\varepsilon_1(0) < 5 \quad (3)$$

However, in our numerical calculation, the static (real) dielectric constants of all the various CNTs having diameter less than 1 nm violate the above inequality as noticed from Tables 1 and 2. This has been also noticed in another first principles calculation [21] of the optical properties of CNTs having diameter 4 Å. Moreover, Eq. (3) indicates infinite static dielectric constants for pure and quasi-metallic CNT. The infinite value is intuitively expected in view of the conducting nature [34] of the available free electrons in CNT. However, we get *finite* positive values for pure and quasi-metallic CNT along with their doped counterparts. We believe that the finiteness of the static values arises due to non-zero positive values of band gaps of all flavors of CNT and the small diameter of the CNT. For quasi-metallic tubes such as (9,0) replacing one of the carbon atoms in hexagonal network by one B atom *always* enhances the static dielectric constant value independent of polarization. In other words, the value of static dielectric susceptibility is increased in doped case for this particular type of CNT. A simple estimation using Eq. (3) based on the plasma frequency and the band gap at Γ point for (7,0) semiconductor CNT predicts 87.22 and 51.58 for pure and doped case, respectively. These values agree quite reasonably with the values for parallel polarization in Table 2. The similar calculation of the (real) static dielectric constant for (9,0) pure tube taking into account the band gap [37] of 0.08 eV yields 6401 that is quite high compared to the ab initio calculation value shown in Table 2. We will come back to this point when we will discuss the loss function of this quasi-metallic system. A substantial order of magnitude of increase of the static dielectric constant in quasi-metallic case is remarkable in all polarization directions even with unpolarized light having incidence direction (1,0,0). This feature of quasi-metallic SWCNT can be used to distinguish it from semiconductor or metallic SWCNT. The reason may be due to presence of small band gap along with the increase of free charge carrier in the doped system.

All the other optical quantities such as reflectivity, refractive index [38] and absorption coefficient can be obtained from the dielectric constant. Below we present the variation of the absorption coefficient and the Loss function that suggests the typical nature of collective excitations of the system.

3.3. Study of the absorption spectra of the doped system

The absorption coefficient α is related to the imaginary part of the dielectric constant as

$$\alpha = \frac{\varepsilon_2\omega}{nc} \quad (4)$$

where n and c are the refractive index and the speed of light, respectively. The absorption spectra depend crucially on the nature of CNT and the direction of polarization. The absorption spectra are limited to UV region only. The existence of peaks in the spectra indicates the maximum absorption at that particular energy. With doping by B atom(s), both the magnitude of the peaks and its position change significantly. The appearance of several peaks in the absorption spectra in perpendicular and unpolarized one makes the analysis little bit complicated. For our convenience, we concentrate on the maximum value of the absorption coefficient in all three cases. We depict in Fig. 6a the dramatic variation in absorption coefficient with doping concentration. A simple polynomial fit for parallel polarization suggests a parabolic type of dependence with doping having a minimum of magnitude $6.48 \times 10^6\ m^{-1}$ at a concentration of 0.40. In other words, for electromagnetic light parallel to axis of (8,0) CNTs, below 0.40 concentration α_{max} *decreases* with doping concentration while above this (0.40) it *increases* with concentration. We also observe the same type of behavior as indicated respectively in Fig. 6a and b for perpendicular

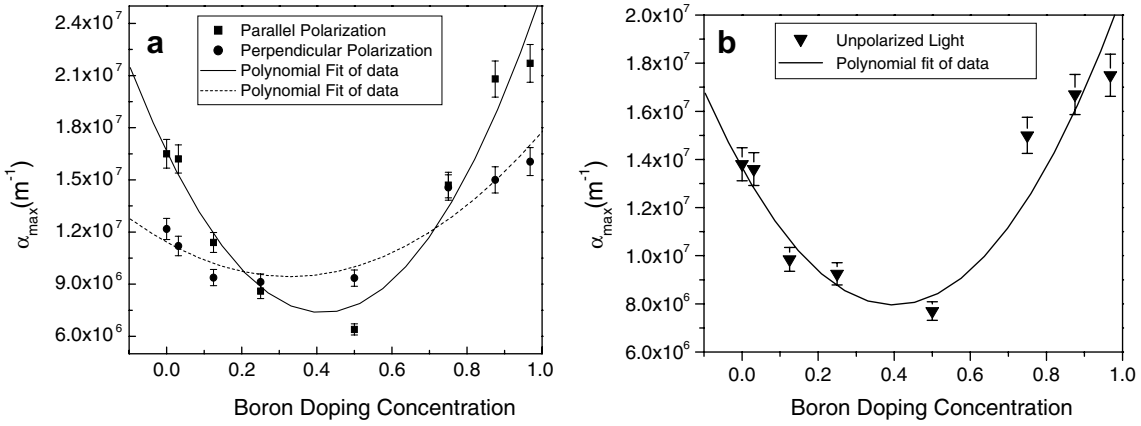

Fig. 6. Variation of the maximum value of the absorption coefficient (α_{max}) with B doping concentration in (a) parallel polarization as well as perpendicular polarization and (b) unpolarized light.

polarization and un-polarized light. We notice in Fig. 6a the maximum value of the absorption coefficient α_{max} ranges from $1.65 \times 10^7\ m^{-1}$ to $2.17 \times 10^7\ m^{-1}$. These values, however, vary for perpendicular as well as unpolarized light. The values of the B doping concentration at which the minimum of α_{max} occurs however differ very slightly from parallel polarization case as shown in Table 3.

3.4. Study of the loss function of the doped system

The loss function, which is a direct measure of the collective excitations of the systems, is defined as $\mathrm{Im}[-1/\varepsilon(q,\omega)]$. Since we are taking the $q \to 0$ limit in our calculation, therefore we are considering the loss function behavior under the long wavelength limit. The peak position of this loss function determines the typical energy of the plasmons in the system. High-resolution transmission electron microscopy (HRTEM) and nano-electron energy loss spectroscopy (nano-EELS) can provide information about the systematics and atomic structural defects of B-doped SWCNTs [39–41]. However, here we are interested in the variation of the peak position as one replaces the carbon atom(s) by B atom(s).

We show in Fig. 7 the typical variation of Loss function for parallel polarization in case of pure and doped semiconductor (8,0) SWNT. Interestingly, we note the appearance of single peak in this pure as well as doped CNT in contrast to multiple peaks in metallic pure and doped system. This represents a unique collective mode of excitation in parallel polarization only. It is also evident from the figure that the magnitude of the peak of the loss function and its position is modified in the doped case. The single peak at 9.73 eV, however, shifts to 9.78 eV on B doping on the CNT. This appearance of single peak (9.5–10 eV) at long wavelength limit ($q \to 0$) may be attributed to the typical *unique* collective excitation of π electrons. This value can be compared with the values [35] obtained for π plasmons at 5.2 eV peak and σ + π plasmons at 21.5 eV for wave vector of 0.15 Å. The shifting of the peak towards lower frequency can be attributed to the reduction of plasma

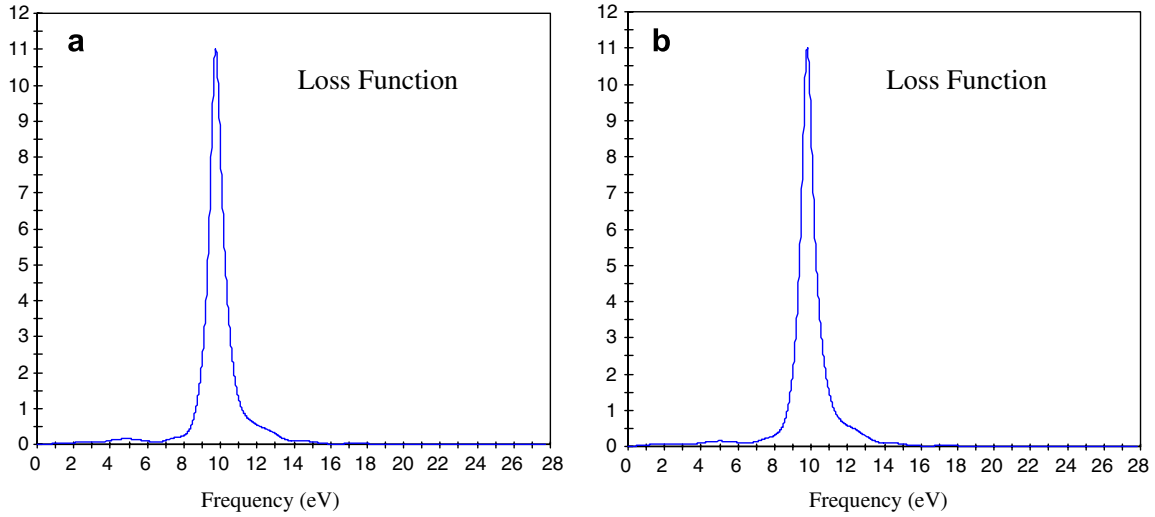

Fig. 7. Loss function of semiconductor (8,0) (a) pure and (b) BC_3 SWNT for parallel polarization.

frequency due to the decrease of total number of electrons on doping. This is evident from the fact that the Fermi energy also decreases with B doping in the system (see Fig. 4a). In perpendicular polarization, the appearance of multiple peaks in the Loss function implies the existence of various collective excitations involving σ and π electrons in the system. This can be taken as one of the characteristic features of *any* type of SWCNTs in perpendicular polarization. Because of the existence of several peaks, it is however difficult to analyze systematically their behavior with doping concentration. The single peak also appears in quasi-metallic (9,0) tube in parallel polarization. For example, in case of quasi-metallic tube (9,0), the pure peak at 9.062 eV is shifted to higher frequency of 9.575 eV upon doping. Even the magnitude of the Loss function is increased in doped case. This may be attributed to increase of free charge carriers. In fact, taking into this plasma resonance frequency and the band gap at Γ point, we find the static dielectric constant for pure and doped case as 21.29 and 92.42, respectively. These values are reasonable with the values shown in Table 1. Thus, we conclude that even a small percentage (3.125%) of B doping can significantly modify the collective excitations of the pure system under various polarization directions.

We depict in Fig. 8, the typical variation of the plasma frequency of doped (8,0) SWNT computed from the Loss function in parallel polarization as well as unpolarized light with the B concentration. Similar to α_{max}, with increase of B doping the plasma resonance frequency first decreases and then increases after some critical concentration. This implies that there exists a unique concentration (~0.44) at which the minimum value of the plasmon frequency is obtained. It may be noted that at the same concentration, both the absorption coefficient as well as the plasmon frequency assume their respective minimum value. In case of unpolarized light, we observe several peaks up to 50% B doping, above this doping, only a single peak with a shoulder. In such a situation, we have concentrated on the main peaks (i.e. peaks having highest magnitude of Loss function) positions up to 50% doping for calculating the plasma resonance frequency. It is to be noted that the minimum value of ω_p and the corresponding B doping do depend on the nature of electromagnetic field. For example, we find the minimum value of the plasma frequency (the corresponding doping concentration) for parallel polarization at 6.94 eV (0.44) while for un-polarized light at 6.64 eV (0.33). The study also demonstrates that the concentration at which the minimum value of ω_p occurs is large in parallel polarization in compared to un-polarized case.

With these plasma frequencies and the band gap at Γ point taken from Fig. 4b, we use Eq. (3) to calculate the static real dielectric constant. However, it is to be remembered that Eq. (3) is strictly valid for *pure* semiconductor SWNT. These computed values are compared in Fig. 9 with simulated ab intio values for parallel polarization. From this figure, we note that Eq. (3) predicts the largest value for pure (8,0) SWCNT while the simulation suggests

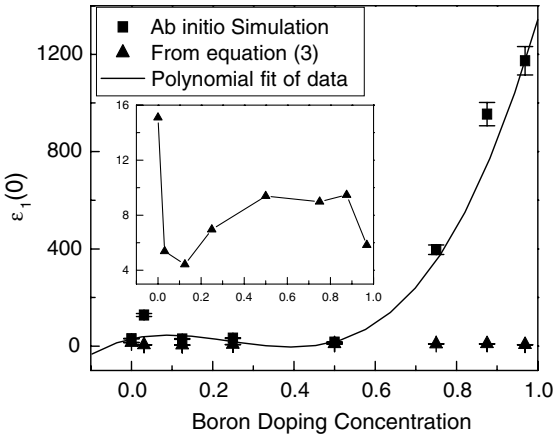

Fig. 9. Comparison of the ab initio static dielectric constant values with Eq. (3). The inset is the expanded version of the values calculated from Eq. (3).

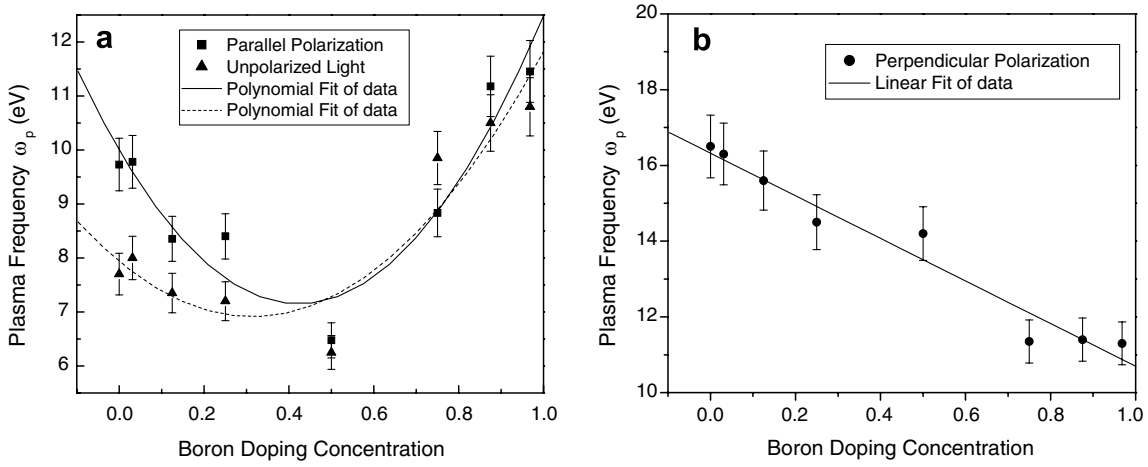

Fig. 8. Variation of the plasma resonance frequency with B doping concentration in (a) parallel polarization as well as for unpolarized light and (b) perpendicular polarization.

the other extreme case i.e. doped one. All the calculated values from Eq. (3) are less than that of the simulations one. Moreover, all these values violate the upper bound restriction as predicted for pure case [36]. Similar behavior has been observed for un-polarized case also. Though the results presented above are based on some specific choice of parameters, however, the qualitative gross features of the optical quantity remain unaltered with the change of parameters.

4. Conclusions and perspectives

From the first principles relaxed C–C bond length DFT calculation of the optical property of B_xC_y SWNT systems, we have observed significant changes in the optical behavior for different CNT systems (radius < 1 nm) with different polarizations. The behavior of the static dielectric constant of B doped system depends on the flavor (nature) of the CNTs. The anisotropy signatures of the dielectric constants noticed in these systems are due to the confined geometry of the CNTs. In all three cases of the incident electromagnetic wave (i.e. parallel polarization, perpendicular polarization and unpolarized light) the maximum value of the absorption coefficient varies significantly with B doping concentration indicating a unique minimum (0.40 for parallel as well as unpolarized while 0.29 for perpendicular one). It is observed that the peak of the loss function in parallel polarization and unpolarized cases shifts to a lower frequency with increasing concentration up to 50% but then shifts to a higher frequency. Also, the non-linear fits to the plasma resonance frequency variation with B concentration indicate the existence of a unique minimum.

Acknowledgements

One of the authors (DJ) would like to thank the National Science Council (NSC) of the Republic of China for financially supporting him as a visiting researcher under Contract No. NSC93-2811-M-002-034. Thanks to Chun-Liang Yeh (IAMS and NCU) for presenting this work in ICON-05 as a poster. Discussions with Dr. C.L. Sun and Dr. Yue-Lin Huang are gratefully acknowledged.

References

[1] Saito R, Dresselhaus G, Dresselhaus MS. Physical properties of carbon nanotubes. London: Imperial College Press; 1998. p. 1–253.
[2] Reich S, Thomsen C, Maulzsch J. Carbon nanotubes: basic concepts and physical properties. Weinheim: Wiley-VCH; 2004. p. 1–211.
[3] Hamada N, Sawada SI, Oshiyama A. New one-dimensional conductors: graphitic microtubules. Phys Rev Lett 1992;68:1579–81.
[4] Yokomichi H, Matoba M, Fukuhara T, Sakima H, Sakai F, Maezawa K. Are boron-doped carbon nanotubes metallic? Phys Stat Solidi (b) 1999;207:R1–2.
[5] Kong J, Franklin N, Zhou C, Chapline M, Peng S, Cho K, et al. Nanotube molecular wires as chemical sensors. Science 2000;287:622–5.
[6] Peng S, Cho K. Ab initio study of doped carbon nanotube sensors. Nano Lett 2003;3:513–7.
[7] Wang R, Zhang D, Zhang Y, Liu C. Boron doped carbon nanotubes serving as a novel chemical sensor for formaldehyde. J Phys Chem B 2006;110:18267–71.
[8] Stephane O, Ajayan PM, Coliex C, Redlich Ph, Lambert JM, Bernier P, et al. Doping graphitic and carbon nanotube structures with boron and nitrogen. Science 1994;266:1683–5.
[9] Sieh WZ, Cherry K, Chopra NG, Blasé X, Miyamoto Y, Rubio A, et al. Synthesis of $B_xC_yN_z$ nanotubules. Phys Rev B 1994;51:11229–32.
[10] Han W, Cumings J, Huang X, Bradley K, Zettl A. Synthesis of aligned $B_xC_yN_z$ nanotubes by a substitution-reaction route. Chem Phys Lett 2001;346:368–72.
[11] Borowiak-Palen E, Pichler T, Fuentes GG, Bendjemil B, Liu X, Graff A, et al. Efficient production of B-substituted single wall carbon nanotubes. Chem Phys Lett 2003;378:516–20.
[12] Borowiak-Palen E, Pichler TB, Liu X, Graff A, Kalenczuk RJ, Knupfer M, et al. Synthesis and electronic properties of B-doped single wall carbon nanotubes. Carbon 2004;42:1123–6.
[13] Yang X, Chen L, Shuai Z, Liu Y, Zhu D. Charge transport behaviour in aligned carbon nanotubes: a quantum chemical investigation. Adv Funct Mater 2004;14(3):289–95.
[14] Picher T, Borowiak-Palen E, Fuentes GG, Knupfer M, Graff A, Fink J, et al. Electronic structure and optical properties of boron doped single wall carbon nanotubes. AIP Conf Proc 2003;685(1):361–5.
[15] Latil S, Roche S, Mayou D, Charlier Jean-Christophe. Mesoscopic transport in chemically doped carbon nanotubes. Phys Rev Lett 2004;92:256805–9.
[16] Liu Yi, Guo H. Current distribution in B- and N-doped carbon nanotubes. Phys Rev B 2004;69:115401–7.
[17] Carroll LD, Redlich P, Blasé X, Charlier J-C, Curran S, Ajayan PM, et al. Effects of nanodomain formation on the electronic structure of doped carbon nanotubes. Phys Rev Lett 1998;81:2332–5.
[18] Czrew R, Terrones M, Charlier J-C, Blasé X, Foley B, Kamalakaran R, et al. Identification of electron donor states in N-doped carbon nanotubes. Nano Lett 2001;1:457–60.
[19] Miyamoto Y, Rubio A, Louie SG, Cohen ML. Electronic properties of tubule forms of hexagonal BC_3. Phys Rev B 1994;50:18360–6.
[20] Fuentes GG, Borowwiak-Palen E, Knupfer M, Pichler T, Fink J, Wirtz L, et al. Formation and electronic properties of BC_3 single-wall nanotubes upon boron substitution of carbon nanotubes. Phys Rev B 2004;69:245403–9.
[21] Machon M, Reich S, Thomsen C, Sanchez-Portal D, Ordejon P. Ab initio calculations of the optical properties of 4-Å-diameter single-walled nanotubes. Phys Rev B 2002;66:155410–5.
[22] Yang XP, Weng HM, Dong J. Optical properties of 4 Å single-walled carbon nanotubes inside zeolite channels studied from first principles calculations. Euro Phys J B 2003;32:345–50.
[23] Liu HJ, Chan CT. Properties of 4 Å carbon nanotubes from first-principles calculations. Phys Rev B 2002;66:115416–20.
[24] Guo GY, Chen KC, Wang Ding-sheng, Duan Chun-gang. Linear and nonlinear optical properties of carbon nanotubes from first-principles calculations. Phys Rev B 2004;69:205416–26.
[25] Segall MD, Lindan PLD, Probert MJ, Pickard CJ, Hasnip PJ, Clark SJ, et al. First-principles simulations: ideas, illustration and the CASTEP code. J Phys Cond Matter 2002;14(11):2717–44.
[26] Payne MC, Teter MP, Allan DC, Arias TA, Joannopoulos JD. Iterative minimization techniques for ab-initio total energy calculations: molecular dynamics and conjugate gradients. Rev Mod Phys 1992;64:1045–97.
[27] Milman V, Winkler B, White JA, Pickard CJ, Payne MC, Akhmatskaya EV, et al. Electronic structure, properties, and phase stability of inorganic crystals: a pseudo potential plane-wave study. Int J Quant Chem 2000;77:895–910.
[28] Perdew JP, Berke K, Ernzerhof M. Generalized gradient approximation made simple. Phys Rev Lett 1996;77:3865–8.
[29] Monkhorst HJ, Pack JD. Special points for Brillouin-zone integrations. Phys Rev B 1992;13:5188–92.
[30] Liu K, Avouris Ph, Martel R, Hsu WK. Electrical transport in doped multiwalled carbon nanotubes. Phys Rev B 2001;63:161404–8.

[31] Wei B, Spolenak R, Kohler-Redlich P, Rühle M, Arzt E. Electrical transport in pure and boron-doped carbon nanotubes. Appl Phys Lett 1999;74:3149–51.
[32] Landau LD, Lifshitz EM. Electrodynamics of continuous media. - New York: Pergamon Press; 1984. p. 58–59.
[33] Jana D, Chen L-C, Chen CW, Chen K-H. Ab initio study of optical conductivity of B_xC_y nano-composite system. Ind J Phys 2007;81: 41–5.
[34] Benedict LX, Louie SG, Cohen ML. Static polarizablities of single-wall carbon nanotubes. Phys Rev B 1995;52:8541–9.
[35] Picher T, Knupfer M, Golden MS, Fink J, Rinzler A, Smalley RE. Localized and delocalized electronic states in single-wall carbon nanotubes. Phys Rev Lett 1998;80:4729–32.
[36] Krupke R, Henrich F, von Löhneysen H, Kappes MM. Separation of metallic from semiconducting single-walled carbon nanotubes. Science 2003;301:344–7.
[37] Ouyang M, Huang JL, Cheung CL, Lieber CM. Energy gaps in metallic single-walled carbon nanotubes. Science 2001;292: 702–5.
[38] Jana D, Chen L-C, Chen CW, Chen K-H. On refractive index and reflectivity of B_xC_y single wall nanotubes: a first principles approach, Asian J Phys, in press.
[39] Gai Pratibha L, Stephane O, McGuire K, Rao Apparao M, Dresselhaus Mildred S, Dresselhaus G, et al. Structural systematics in boron-doped single wall carbon nanotubes. J Mater Chem 2004;14:669–75.
[40] Graff A, Gemming T, Borowiak-Palen E, Ritschel M, Picher T, Knupfer M, et al. Analytical TEM investigation of B doped carbon and BN nanotubes. Microsc Microannal 2003;9:178–9.
[41] Borowiak-Palen E, Picher T, Fuentes GG, Graff A, Kalenczuk RJ, Knupfer M, et al. Production and characterization of MWBNNT and B-doped SWCNT. AIP Conf Proc 2003;685(1):374–7.